# Performance Analysis on Airfoil Model in Wind Tunnel Testing Machine (WTTM)

## Ishan.M.Shah[1], S. A. Thakkar[2], K. H. Thakkar[3], Bhavesh A. Patel[4]

(ME Student, Department of Mechanical Engineering, Sankalchand Patel College of Engineering, Visnagar, Gujarat, India)[1,4]
(Assistant Professor, Department of Mechanical Engineering, Sankalchand Patel College of Engineering, Visnagar, Gujarat, India)[2,3]

## ABSTRACT

A Wind Tunnel Testing Machine (WTTM) is a tool used in Aerodynamic research to study the effects of Air moving past to the solid objects. A wind tunnel testing machine consists of a closed tubular passage with the object under test mounted in the middle and powerful fan system moves air past to the object. The wing (airfoil) provides lift by creating a situation where the pressure above the wing is lower than the pressure below the wing. Since the pressure below the wing is higher than the pressure above the wing. The readings has been taken on airfoil model in Wind Tunnel Testing Machine (WTTM) at different air velocity 20m/sec, 25m/sec, 30m/sec and different angle of attack $0^0,5^0,10^0,15^0,20^0$. Air velocity and pressures are measured in several ways in wind tunnel testing machine by use to measuring instruments like Anemometer and Multi tube manometer. The Surface roughness of an airfoil is can be measure by Surface roughness tester. The heat signature of a testing model is can be measure by Thermal Imaging Camera. The CFD analysis is also carried out at various sections of airfoil angles and velocity. The maximum performance to the airfoil model is achieved at $10^0$ on angle of attack.

## I. INTRODUCTION

### 1.1 Wind Tunnel

A wind tunnel is a tool use in Aerodynamic research to study the effects of Air moving past to the solid objects.
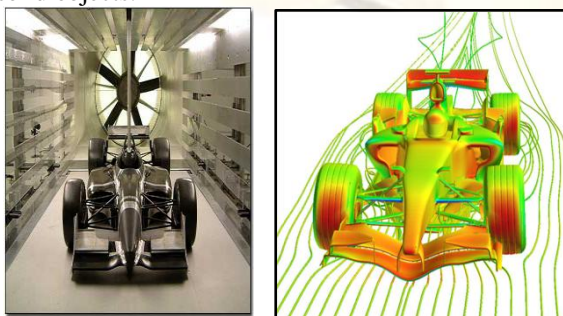


*Fig 1 Wind Tunnel Machine*

A wind tunnel consists of a closed tubular passage with the object under test mounted in the middle and powerful fan system moves air past to the object.

### 1.2 AIRFOIL

The airplane generates lift using its wings, the cross sectional shape of the wing is called an airfoil. An airfoil (in American English) or aerofoil (in British English) is the shape of a wing or blade.
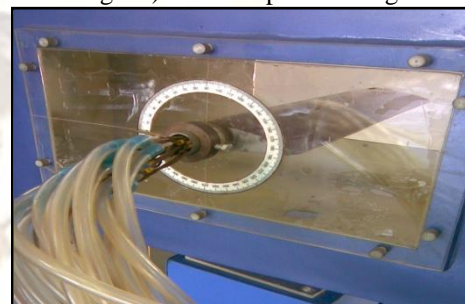


*Fig 2 Airfoil Testing Model*

### 1.3 Angle Of Attack

Angle of attack is the angle between the body's reference line and the oncoming flow.



*Fig 3 Airfoil Model*

### 1.4 Light Airplanes

The takeoff and landing speed to a many light airplanes is 40 knots (72 km/h, 20 m/sec) to 55 knots (101 km/h, 28 m/sec).



*Fig 4 Light Airplanes*

The takeoff speed is usually dependant on the airplane weight, the heavier the weight, the greater speed needed. Some aircraft are specifically designed for short takeoff and landing, which they achieve by becoming airborne at very low speed.

### 1.5 Computational Fluid Dynamics (CFD) Analysis

Computational fluid dynamics is a branch of fluid mechanics that uses numerical methods and algorithms to solve and analyze problems that involve fluid flows. Computers are used to perform the calculations required to simulate the interaction of liquids and gases with surfaces defined by boundary conditions.

## II.     EXPERIMENTAL DETAILS
### 2.1 INTRODUCTION



*Fig 5 Wind Tunnel Testing Machine (WTTM)*

Air velocity through the test section is determined by anemometer and all its readings are taken. Pressure readings on airfoil test model can determine by multi tube manometer. Smoke can be introduced in to the airflow upstream of the test model, and their path around the model can be photographed.

### 2.2 EXPERIMENTAL SETUP
### 2.2.1 WIND TUNNEL COMPONENTS
### (i) ENTRY SECTION

The entry is shaped to guide the air smoothly into the tunnel. Proper flow separation here would give excessive turbulence and non uniformity in velocity in the working section. So 2 to 2.5 meter air space is required to entry. The entry section is followed by a settling chamber which leads to be contraction to get velocity increase, which is connected with working section. Contraction is a specially designed carved due to give good results in test section. The setting chamber usually includes a honeycomb.



*Fig 6 Entry Section*

### (ii) WORKING SECTION



*Fig 7 Working Section*

It is also called test section as we can fit the models and use this space for experimentation. Wind Tunnel is having 300 mm x 300 mm test section with 1 meter length and two windows to insert the models.

### (iii) DIFFUSER SECTION



*Fig 8 Diffuser Section*

The working section is followed by a divergent duct. The divergence results in a corresponding reduction in the flow speed. Diffuser reduces in dynamic pressure leads to reduction in power losses at the exit. Leaving the diffuser, the air enters the lab, along which it flows slowly to get this retardation 2 meters air space is to be provided.

### (iv) FAN AND DRIVE



*Fig 9 Fan and Drive*

A six blade fan is fitted to a sturdy frame work and is coupled to a Motor. This motor is controlled with a variable frequency. Digital display which gives smooth variation of air velocity in test section which can be seen on anemometer and one can set the velocity of Air to desired value.

### 2.2.2 WIND TUNNEL SPECIFICATION

Working Section Material: Acrylic Sheet 10 mm Thick

Blower Fan:                         6 Blades, M.S. Fan
A.C. Motor:                         5 H.P, 3000 RPM
Frequency Drive Controller:   High Frequency Inverter
Make:                               "TOSHIBA",   MINIELEC MAKE
Model: 400 V, Class VFS7 4037P, 3.7 k w VFD
Air velocity in test section: 3 to 30 m/sec
Duct Material:                     Fiber Reinforced Plastic
Air length:                         9.5 meter
Contraction ratio:               9: 1

### 2.2.3 MEASURING INSTRUMENTS

Air velocity and pressures are measured in several ways in wind tunnel.

### (i) ANEMOMETER

An anemometer measures the air speed in wind tunnel. An anemometer is a device for measuring wind speed, and the term is derived from the Greek word anemos, meaning wind, and is used to describe any airspeed measurement instrument used in meteorology or aerodynamics. The first known description of an anemometer was given by Leon Battista Alberti around year 1450.



*Fig 10 Anemometer*

In the anemometer the pressure is measured, although the scale is usually graduated as a velocity scale. In cases where the density of the air is significantly different from the calibration value (as on a high mountain) an allowance must be made.

### (ii) MANOMETER

The multi tube manometer consists of 16 manometers with a mm scale mounted on a swiveling panel. Water is supplied to the manometers centrally from a water reservoir. This instrument provides multipoint pressure measuring facility. An element corresponds to the pressure at a point. It consists of a reservoir for the manometer liquid open to the atmospheric pressure. The reservoir is connected to a number of tubes at the bottom where all the tubes are the points of interest at which pressure is to be measured.



*Fig 11 Manometer*

There are 16 tubes of the same length, connections provided to these tubes for connecting the tubes of the other tube coming from the point of interest. Pressures are measured relative to atmospheric datum.

### (iii) SURFACE ROUGHNESS TESTER

Surface roughness tester can measure the texture of an airfoil surface in wind tunnel. It is quantified by the vertical deviations of a real surface from its ideal form. If these deviations are large, the surface is rough; if they are small the surface is smooth. Surface roughness is typically considered to be the high frequency, short wavelength component of a measured surface.



*Fig 12 Surface Roughness Tester*

Surface roughness plays an important role in determining how a real object will interact with its environment. Rough surfaces usually wear more quickly and have higher friction coefficients than smooth surfaces. Surface roughness is typically measured in micro inches.

### (iv) THERMAL IMAGING CAMERA

Thermal Imaging Camera can be used to see the heat signature of an airfoil testing model in wind tunnel. A Thermal Imaging Camera is a device that forms an image using infrared radiation, similar to a common camera that forms an image using visible

light. A Thermal Imaging Camera is a type of thermo graphic camera.

*Fig 13 Thermal Imaging Camera*

A Thermal Imaging Camera consists of five components: an optic system, detector, amplifier, signal processing, and display. Thermal imaging cameras incorporate these components in a heat resistant, ruggedized, and waterproof housing. These parts work together to infrared radiation, such as that given by warm objects or flames, in to a visible light representation in real time.

### 2.2.4 AIRFOIL TESTING MODEL READINGS

The readings have been taken on airfoil model in Wind Tunnel Testing Machine (WTTM) at different air velocity 20m/sec, 25m/sec, 30m/sec and different angle of attack $0^0, 5^0, 10^0, 15^0, 20^0$.

| Angle Number | Angle of Attack $\alpha$ | Manometer Readings (cm) 20 m/sec | | | | | | | | | | | | | | | |
|---|---|---|---|---|---|---|---|---|---|---|---|---|---|---|---|---|---|
| | | 1 | 2 | 3 | 4 | 5 | 6 | 7 | 8 | 9 | 10 | 11 | 12 | 13 | 14 | 15 | 16 |
| 1 | $0^0$ | 13.5 | 16.3 | 18.2 | 17.9 | 17.1 | 17.3 | 16.2 | 15.7 | 14.9 | 16.0 | 17.0 | 16.0 | 15.8 | 15.6 | 15.5 | 15.6 |
| 2 | $5^0$ | 14.4 | 17.2 | 18.7 | 18.2 | 17.4 | 17.0 | 16.2 | 15.7 | 15.0 | 15.4 | 16.5 | 15.7 | 15.5 | 15.5 | 15.4 | 15.5 |
| 3 | $10^0$ | 16.0 | 18.0 | 19.0 | 18.3 | 17.6 | 16.7 | 16.0 | 15.6 | 15.0 | 14.4 | 15.6 | 15.2 | 15.2 | 15.2 | 15.2 | 15.5 |
| 4 | $15^0$ | 18.6 | 18.8 | 19.3 | 18.2 | 16.8 | 16.4 | 15.8 | 15.5 | 15.4 | 14.0 | 15.0 | 14.8 | 14.8 | 15.0 | 15.2 | 15.5 |
| 5 | $20^0$ | 21.0 | 19.7 | 19.6 | 17.5 | 15.9 | 16.3 | 16.2 | 16.4 | 16.0 | 13.4 | 14.5 | 14.2 | 14.5 | 14.7 | 15.0 | 15.5 |
| Default Readings | | 15.5 | 15.5 | 15.9 | 15.8 | 15.5 | 16.0 | 16.0 | 16.0 | 15.9 | 16.1 | 16.3 | 15.8 | 15.8 | 16.0 | 16.0 | 16.0 |

**Table 1 Manometer Readings (cm) at 20 m/sec Velocity**

| Angle Number | Angle of Attack $\alpha$ | Manometer Readings (cm) 25 m/sec | | | | | | | | | | | | | | | |
|---|---|---|---|---|---|---|---|---|---|---|---|---|---|---|---|---|---|
| | | 1 | 2 | 3 | 4 | 5 | 6 | 7 | 8 | 9 | 10 | 11 | 12 | 13 | 14 | 15 | 16 |
| 1 | $0^0$ | 11.5 | 16.1 | 18.5 | 18.5 | 17.6 | 17.5 | 16.2 | 15.5 | 14.5 | 16.7 | 17.9 | 16.4 | 15.9 | 15.6 | 15.5 | 15.5 |
| 2 | $5^0$ | 13.0 | 17.2 | 19.2 | 18.9 | 17.9 | 17.4 | 16.2 | 15.5 | 14.5 | 15.5 | 16.9 | 16.0 | 15.5 | 15.4 | 15.3 | 15.4 |
| 3 | $10^0$ | 16.2 | 19.0 | 20.2 | 19.2 | 18.2 | 17.0 | 16.0 | 15.4 | 14.7 | 13.7 | 15.4 | 14.9 | 14.8 | 14.9 | 14.9 | 15.2 |
| 4 | $15^0$ | 19.0 | 20.0 | 20.7 | 19.4 | 17.6 | 16.7 | 15.9 | 15.3 | 14.7 | 13.1 | 14.7 | 14.3 | 14.4 | 14.6 | 14.6 | 15.2 |
| 5 | $20^0$ | 22.0 | 20.2 | 20.5 | 18.5 | 16.0 | 16.2 | 16.2 | 16.2 | 15.7 | 12.7 | 14.0 | 13.9 | 14.2 | 14.4 | 14.6 | 15.3 |
| Default Readings | | 15.5 | 15.5 | 15.9 | 15.8 | 15.5 | 16.0 | 16.0 | 16.0 | 15.9 | 16.1 | 16.3 | 15.8 | 15.8 | 16.0 | 16.0 | 16.0 |

**Table 2 Manometer Readings (cm) at 25 m/sec Velocity**

| Angle Number | Angle of Attack α | Manometer Readings (cm) 30 m/sec | | | | | | | | | | | | | | | |
|---|---|---|---|---|---|---|---|---|---|---|---|---|---|---|---|---|---|
| | | 1 | 2 | 3 | 4 | 5 | 6 | 7 | 8 | 9 | 10 | 11 | 12 | 13 | 14 | 15 | 16 |
| 1 | $0^0$ | 11.0 | 17.0 | 20.7 | 20.3 | 18.9 | 18.3 | 16.3 | 15.0 | 13.2 | 16.6 | 19.0 | 17.0 | 15.7 | 15.4 | 14.9 | 14.7 |
| 2 | $5^0$ | 12.5 | 20.0 | 22.9 | 21.2 | 19.5 | 17.4 | 16.0 | 14.7 | 13.3 | 13.3 | 16.9 | 15.9 | 15.0 | 14.7 | 14.5 | 14.7 |
| 3 | $10^0$ | 17.0 | 22.0 | 23.4 | 21.2 | 18.9 | 17.3 | 16.0 | 15.2 | 13.9 | 11.0 | 15.0 | 14.7 | 14.3 | 14.2 | 14.2 | 14.4 |
| 4 | $15^0$ | 23.0 | 22.5 | 23.0 | 19.0 | 16.4 | 16.7 | 16.6 | 16.5 | 15.4 | 9.9 | 13.4 | 13.7 | 13.9 | 14.0 | 14.4 | 15.1 |
| 5 | $20^0$ | 26.3 | 21.5 | 20.5 | 16.5 | 16.0 | 16.9 | 16.9 | 17.4 | 16.8 | 9.9 | 12.8 | 13.3 | 15.7 | 14.0 | 14.7 | 16.0 |
| Default Readings | | 15.5 | 15.5 | 15.9 | 15.8 | 15.5 | 16.0 | 16.0 | 16.0 | 15.9 | 16.1 | 16.3 | 15.8 | 15.8 | 16.0 | 16.0 | 16.0 |

**Table 3 Manometer Readings (cm) at 30 m/sec Velocity**

## III.    SOFTWARE ANALYSIS

Software testing is an investigation conducted to provide information about the performance of the product or model under test. Computational Fluid Dynamics (CFD) is a computer based mathematical modeling tool that can be experimentation in the field of fluid flow and heat transfer.

Computational fluid dynamics, usually CFD, is a branch of fluid mechanics that uses numerical methods and algorithms to solve and analyze the involved fluid flows. Computers are used to perform the calculations required to simulate the interaction of liquids or gases with surfaces defined by boundary conditions.
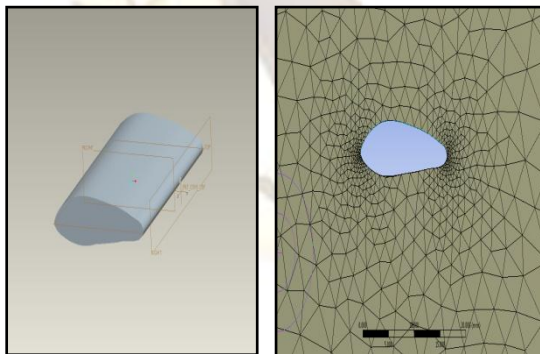


*Fig 14 Pro/E Model and its Meshing*

ANSYS 14.5 software has been used to analyze the airfoil model. The readings of airfoil model at different air velocity 20m/sec, 25m/sec, 30m/sec and different angle of attack $0^0$, $5^0$,$10^0$, $15^0$, $20^0$ have been taken. Air pressure and velocity streamlines are shown in figures at different angles and velocity.

**3.1  Air Pressure and Velocity Streamlines at $0^0$ Angle of Attack**

At $0^0$ angle of attack CFD analysis show that the pressure differences at both sides on airfoil model is very small and it is match with practical readings.
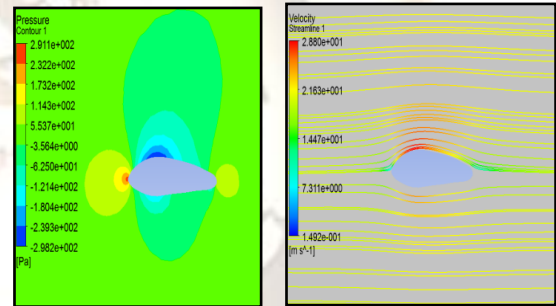


*Fig 15 Air Pressure and Velocity Streamlines at 20 m/sec Velocity*
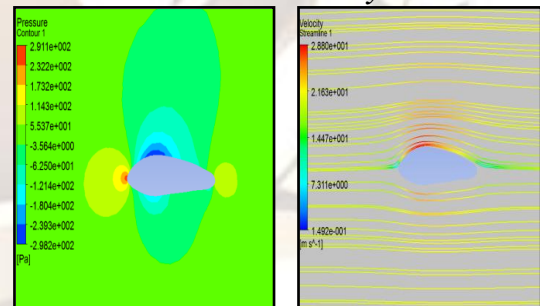


*Fig 16 Air Pressure and Velocity Streamlines at 25 m/sec Velocity*
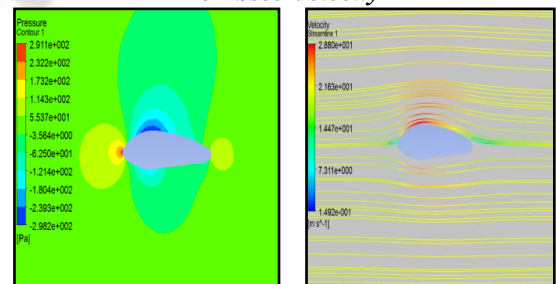


*Fig 17 Air Pressure and Velocity Streamlines at 30 m/sec Velocity*

### 3.2 Air Pressure and Velocity Streamlines at $5^0$ Angle of Attack

At $5^0$ angle of attack, CFD analysis shows that the pressure differences at both sides on airfoil model is very small and it is match with practical readings.
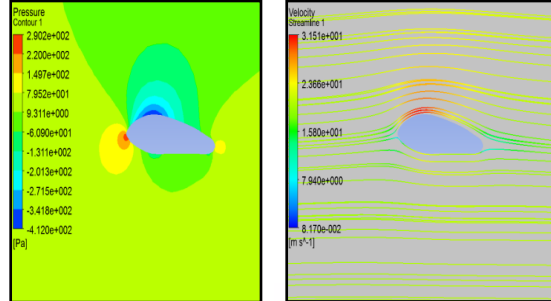


*Fig 18 Air Pressure and Velocity Streamlines at 20 m/sec Velocity*
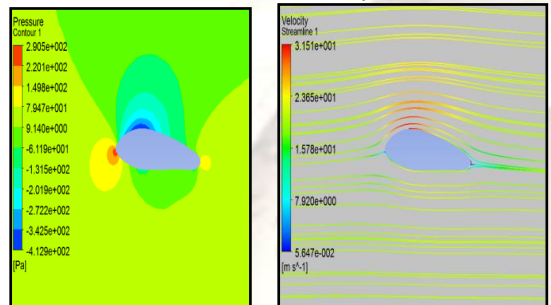


*Fig 19 Air Pressure and Velocity Streamlines at 25 m/sec Velocity*
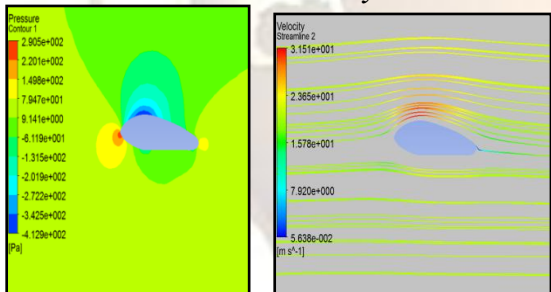


*Fig 20 Air Pressure and Velocity Streamlines at 30 m/sec Velocity*

### 3.3 Air Pressure and Velocity Streamlines at $10^0$ Angle of Attack

At $10^0$ angle of attack CFD analysis show that the bottom surfaces pressure is higher compare to upper surfaces on the airfoil and it is match with practical readings.
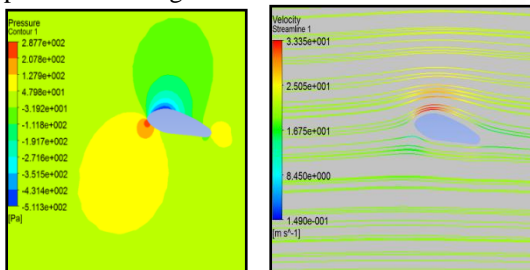


*Fig 21 Air Pressure and Velocity Streamlines at 20 m/sec Velocity*
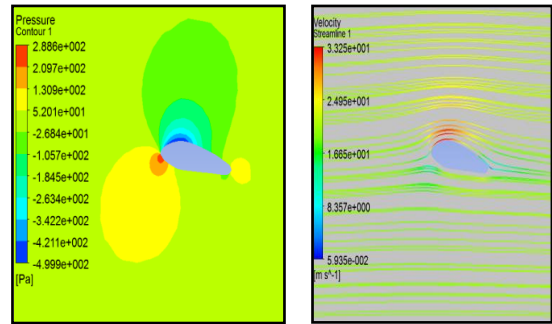


*Fig 22 Air Pressure and Velocity Streamlines at 25 m/sec Velocity*
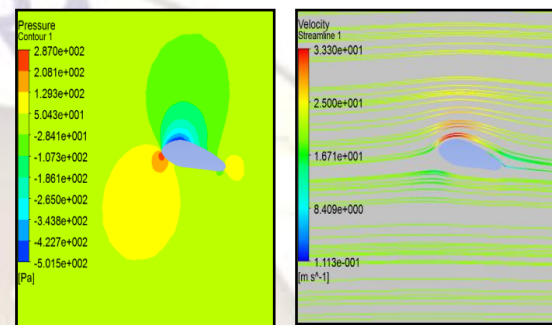


*Fig 23 Air Pressure and Velocity Streamlines at 30 m/sec Velocity*

### 3.4 Air Pressure and Velocity Streamlines at $15^0$ Angle of Attack

At $15^0$ angle of attack CFD analysis show that the bottom surfaces pressure is higher compare to upper surfaces on the airfoil but it is higher pressure differences and it is match with practical readings.
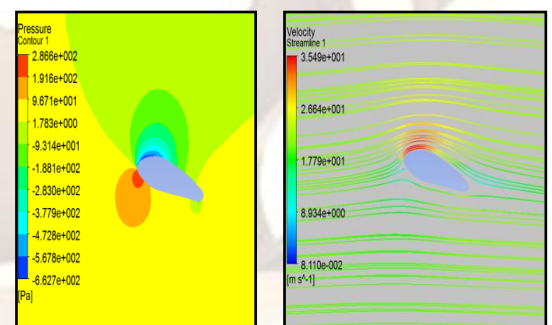


*Fig 24 Air Pressure and Velocity Streamlines at 20 m/sec Velocity*
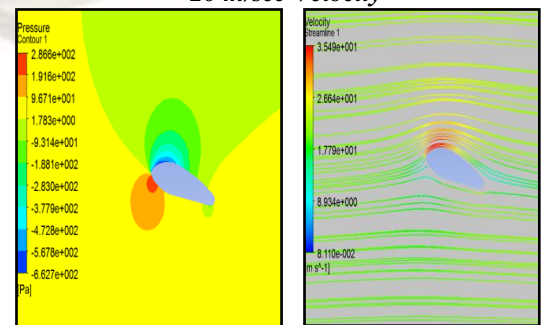


*Fig 25 Air Pressure and Velocity Streamlines at 25 m/sec Velocity*
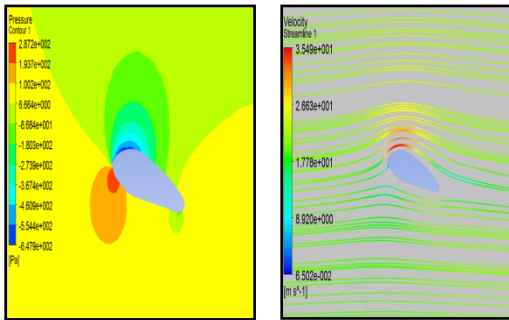
*Fig 26 Air Pressure and Velocity Streamlines at 30 m/sec Velocity*
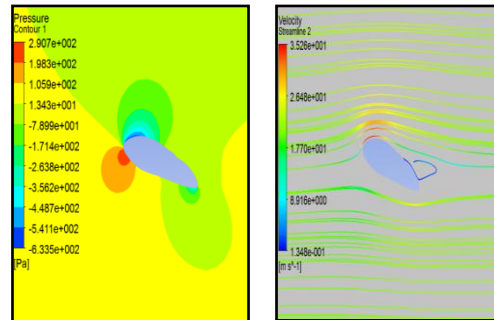
**3.5  Air Pressure and Velocity Streamlines at 20$^0$ Angle of Attack**

  At 20$^0$ angle of attack CFD analysis show that bottom surfaces pressure is higher compare to upper surfaces on the airfoil but it is also higher pressure differences and it is match with practical readings.



*Fig 27 Air Pressure and Velocity Streamlines at 20 m/sec Velocity*
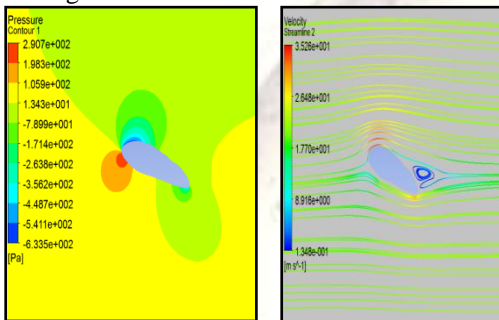


*Fig 28 Air Pressure and Velocity Streamlines at 25 m/sec Velocity*
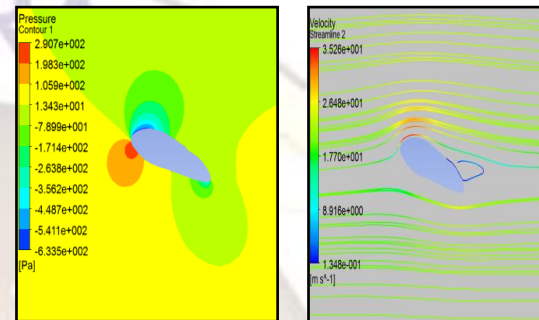


*Fig 29 Air Pressure and Velocity Streamlines at 30 m/sec Velocity*

## IV. RESULTS AND DISCUSSION

  The readings have been taken on airfoil model on Wind Tunnel Testing Machine (WTTM) at different air velocity 20m/sec, 25m/sec, 30m/sec and different angle of attack 0$^0$, 5$^0$, 10$^0$, 15$^0$, 20$^0$. Practically air pressure and velocity readings are taken on wind tunnel and shown in charts. The CFD analysis is also done in ANSYS 14.5 software at various sections to airfoil angles and velocity.

### 4.1  AIRFOIL TESTING MODEL CHARTES

  The 0$^0$ angle of attack creates pressure at both side on airfoil model but pressure different is very small and curve obtained is not smooth.



| | 1 | 2 | 3 | 4 | 5 | 6 | 7 | 8 | 9 | 10 | 11 | 12 | 13 | 14 | 15 | 16 |
|---|---|---|---|---|---|---|---|---|---|---|---|---|---|---|---|---|
| Series1 | 13.5 | 16.3 | 18.2 | 17.9 | 17.1 | 17.3 | 16.2 | 15.7 | 14.9 | 16 | 17 | 16 | 15.8 | 15.6 | 15.5 | 15.6 |
| Series2 | 11.5 | 16.1 | 18.5 | 18.5 | 17.6 | 17.5 | 16.2 | 15.5 | 14.5 | 16.7 | 17.9 | 16.4 | 15.9 | 15.6 | 15.5 | 15.5 |
| Series3 | 11 | 17 | 20.7 | 20.3 | 18.9 | 18.3 | 16.3 | 15 | 13.2 | 16.6 | 19 | 17 | 15.7 | 15.4 | 14.9 | 14.7 |
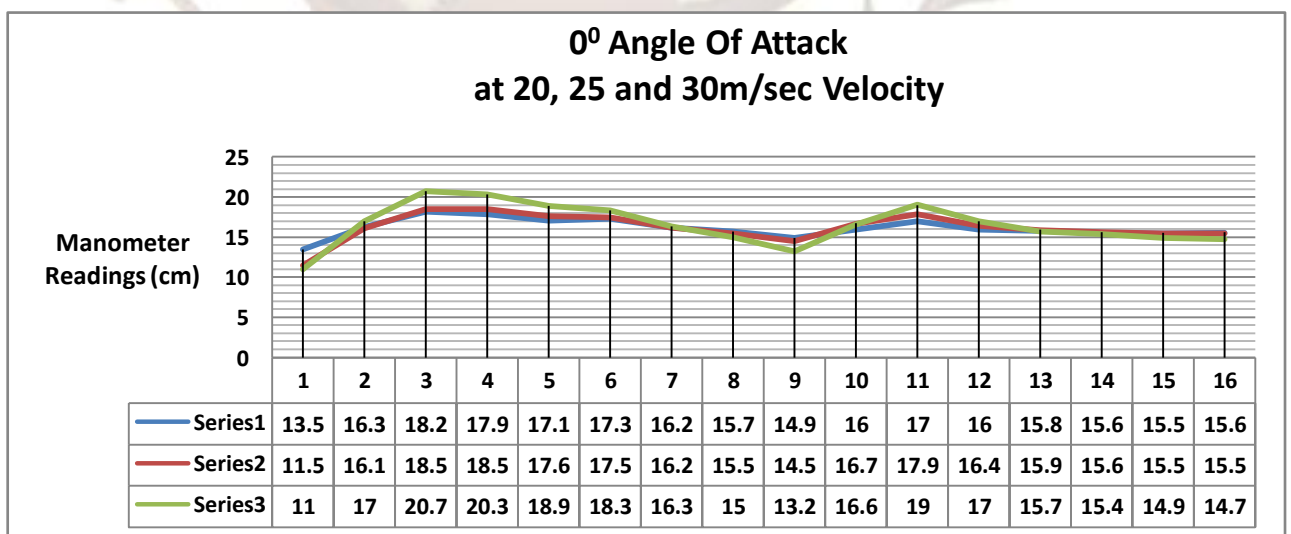
*Fig 30 0$^0$ Angle Of Attack at 20, 25 and 30m/sec Velocity*

The $5^0$ angle of attack is all so create the pressure at both side on airfoil model but pressure different is very small and curve is not smooth at different air velocity.

### $5^0$ Angle Of Attack at 20, 25 and 30m/sec Velocity

| | 1 | 2 | 3 | 4 | 5 | 6 | 7 | 8 | 9 | 10 | 11 | 12 | 13 | 14 | 15 | 16 |
|---|---|---|---|---|---|---|---|---|---|---|---|---|---|---|---|---|
| Series1 | 14.4 | 17.2 | 18.7 | 18.2 | 17.4 | 17 | 16.2 | 15.7 | 15 | 15.4 | 16.5 | 15.7 | 15.5 | 15.5 | 15.4 | 15.5 |
| Series2 | 13 | 17.2 | 19.2 | 18.9 | 17.9 | 17.4 | 16.2 | 15.5 | 14.5 | 15.5 | 16.9 | 16 | 15.5 | 15.4 | 15.3 | 15.4 |
| Series3 | 12.5 | 20 | 22.9 | 21.2 | 19.5 | 17.4 | 16 | 14.7 | 13.3 | 13.3 | 16.9 | 15.9 | 15 | 14.7 | 14.5 | 14.7 |
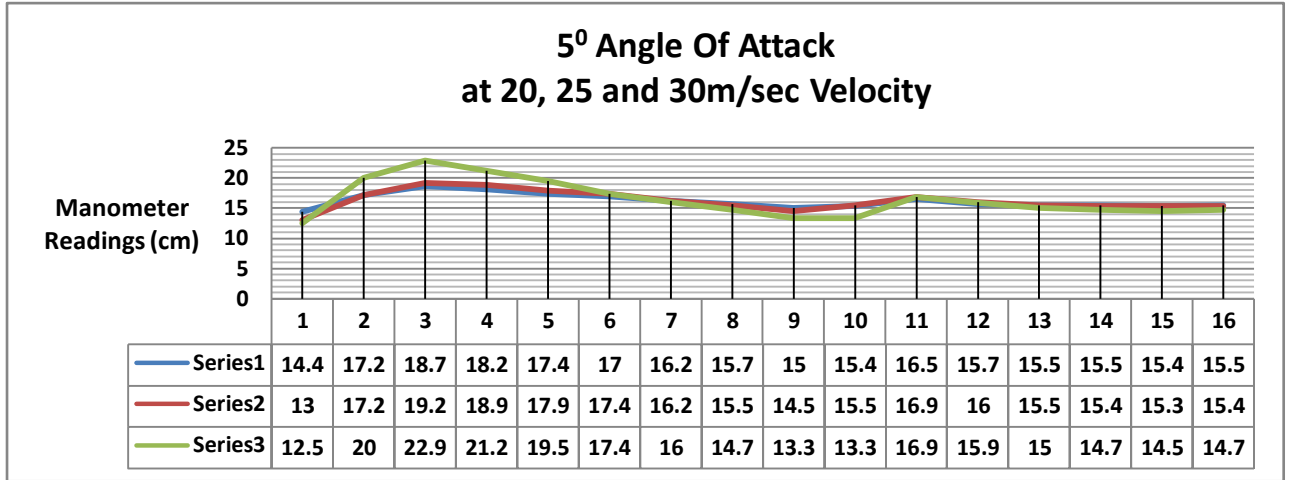
*Fig 31 $5^0$ Angle Of Attack at 20, 25 and 30m/sec Velocity*

The wind tunnels air pressure and velocity $10^0$ angle of attack readings charts shown that the maximum performance of the airfoil model is achieved at $10^0$ on angle of attack and curve is achieve smooth at different air velocity.

### $10^0$ Angle Of Attack at 20, 25 and 30m/sec Velocity

| | 1 | 2 | 3 | 4 | 5 | 6 | 7 | 8 | 9 | 10 | 11 | 12 | 13 | 14 | 15 | 16 |
|---|---|---|---|---|---|---|---|---|---|---|---|---|---|---|---|---|
| Series1 | 16 | 18 | 19 | 18.3 | 17.6 | 16.7 | 16 | 15.6 | 15 | 14.4 | 15.6 | 15.2 | 15.2 | 15.2 | 15.2 | 15.5 |
| Series2 | 16.2 | 19 | 20.2 | 19.2 | 18.2 | 17 | 16 | 15.4 | 14.7 | 13.7 | 15.4 | 14.9 | 14.8 | 14.9 | 14.9 | 15.2 |
| Series3 | 17 | 22 | 23.4 | 21.2 | 18.9 | 17.3 | 16 | 15.2 | 13.9 | 11 | 15 | 14.7 | 14.3 | 14.2 | 14.2 | 14.4 |
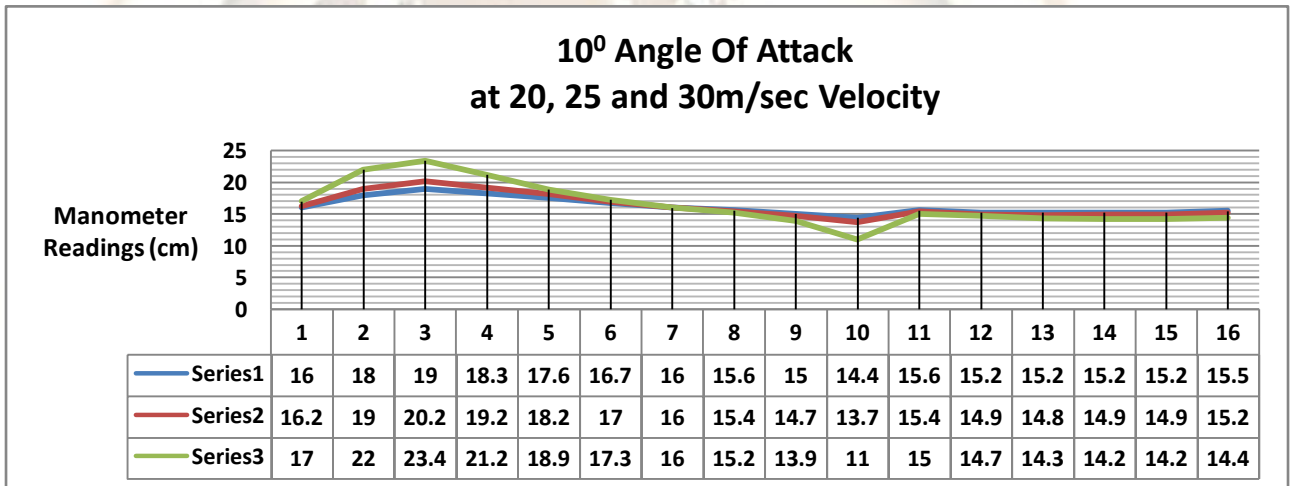
*Fig 32 $10^0$ Angle Of Attack at 20, 25 and 30m/sec Velocity*

The $15^0$ angle of attack is creating the pressure at bottom surfaces but the pressure curve is not smooth at different air velocity.

### $15^0$ Angle Of Attack at 20, 25 and 30m/sec Velocity

| | 1 | 2 | 3 | 4 | 5 | 6 | 7 | 8 | 9 | 10 | 11 | 12 | 13 | 14 | 15 | 16 |
|---|---|---|---|---|---|---|---|---|---|---|---|---|---|---|---|---|
| Series1 | 18.6 | 18.8 | 19.3 | 18.2 | 16.8 | 16.4 | 15.8 | 15.5 | 15.4 | 14 | 15 | 14.8 | 14.8 | 15 | 15.2 | 15.5 |
| Series2 | 19 | 20 | 20.7 | 19.4 | 17.6 | 16.7 | 15.9 | 15.3 | 14.7 | 13.1 | 14.7 | 14.3 | 14.4 | 14.6 | 14.6 | 15.2 |
| Series3 | 23 | 22.5 | 23 | 19 | 16.4 | 16.7 | 16.6 | 16.5 | 15.4 | 9.9 | 13.4 | 13.7 | 13.9 | 14 | 14.4 | 15.1 |
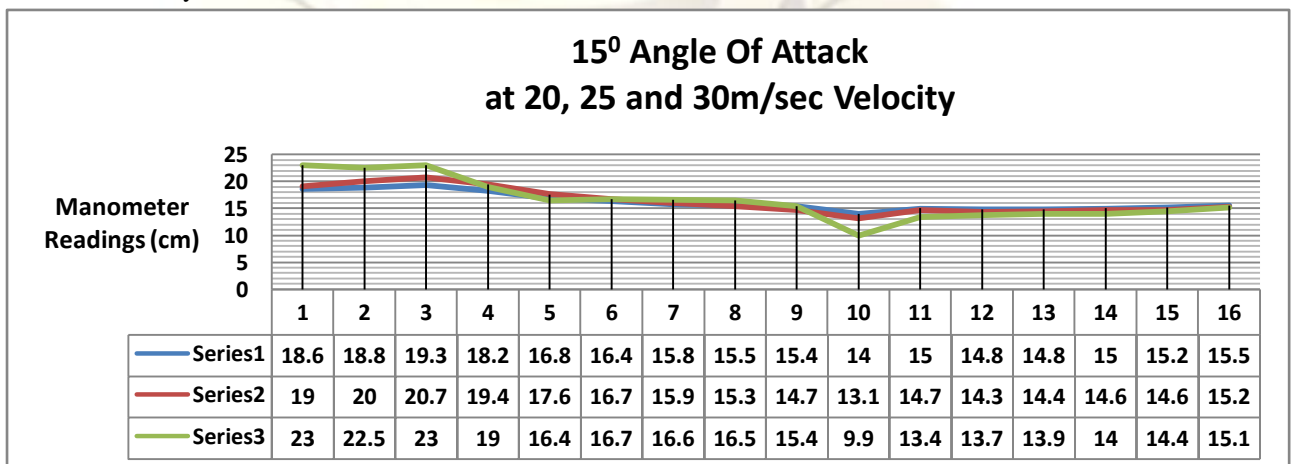
*Fig 33 $15^0$ Angle Of Attack at 20, 25 and 30m/sec Velocity*

The $20^0$ angle of attack is creating the higher pressure at bottom surfaces but the pressure curve is not smooth at different air velocity.

## $20^0$ Angle Of Attack at 20, 25 and 30m/sec Velocity

| | 1 | 2 | 3 | 4 | 5 | 6 | 7 | 8 | 9 | 10 | 11 | 12 | 13 | 14 | 15 | 16 |
|---|---|---|---|---|---|---|---|---|---|---|---|---|---|---|---|---|
| Series1 | 21 | 19.7 | 19.6 | 17.5 | 15.9 | 16.3 | 16.2 | 16.4 | 16 | 13.4 | 14.5 | 14.2 | 14.5 | 14.7 | 15 | 15.5 |
| Series2 | 22 | 20.2 | 20.5 | 18.5 | 16 | 16.2 | 16.2 | 16.2 | 15.7 | 12.7 | 14 | 13.9 | 14.2 | 14.4 | 14.6 | 15.3 |
| Series3 | 26.3 | 21.5 | 20.5 | 16.5 | 16 | 16.9 | 16.9 | 17.4 | 16.8 | 9.9 | 12.8 | 13.3 | 15.7 | 14 | 14.7 | 16 |

Manometer Readings (cm)
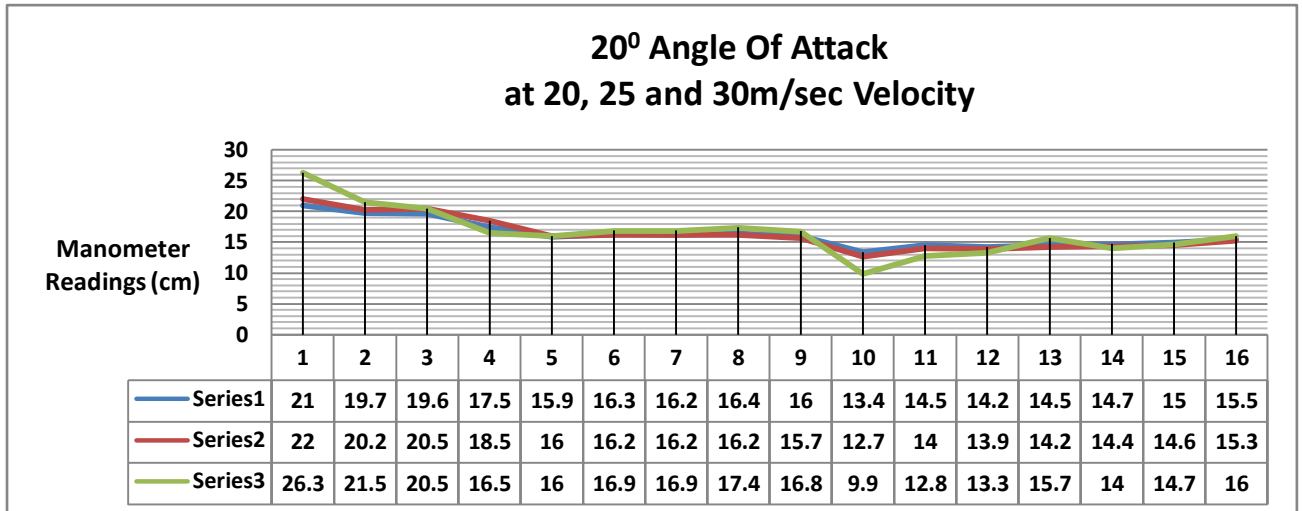
*Fig 34 $20^0$ Angle Of Attack at 20, 25 and 30m/sec Velocity*

The Wind Tunnel Testing Machine (WTTM) air pressure and velocity readings charts show that the maximum performance of the airfoil model has been achieved at $10^0$ angle of attack.

## V. CONCLUSIONS

The readings have been taken on airfoil model in Wind Tunnel Testing Machine (WTTM) at different air velocity 20 m/sec, 25 m/sec, 30m/sec and different angle of attack $0^0$, $5^0$, $10^0$, $15^0$, $20^0$. The airfoil provides lift by creating a situation where the pressure above the airfoil is lower than the pressure below the airfoil. Since the pressure below the airfoil is higher than the pressure above the airfoil. The wind tunnels air pressure and velocity readings charts shown that the maximum performance of the airfoil model is achieved at $10^0$ on angle of attack. The CFD analyses are also done in software at various sections of airfoil angles and velocity. The maximum performance to the airfoil model is achieved at $10^0$ on angle of attack…..

## VI. FUTURE WORK

An airfoil can be designed specifically for airfoil testing on wind tunnel so that a better measurement system can be achieved and the angle of attack and air flow velocity may be varied to improve the performance of different airfoils. A proper means for construction of airfoils could be utilized for further analysis.

## REFERENCES

[1] A. Cigada, M. Falco, A. Zasso (Departimento di Meccanica, Politecnico di Milano, Milano, Italy) Development of new systems to measure the aerodynamic forces on section models in wind tunnel testing. Journal of Wind Engineering and Industrial Aerodynamics 89 (2001) 725-746.

[2] Christoph Fritzsche, Thomas Geyer, Jens Giesler (Institut Verkehrstechnik, Brandenburgische Technische Universität, Cottbus, Germany) Acoustic and aerodynamic design and characterization of a small scaleaeroacoustic wind tunnel. Applied Acoustics 70 (2009) 1073-1080.

[3] Hyeok bin Kwon, Young Whe Park, Moon Sang Kim (Department of Aerospace Engineering, Seoul National University, Seoul, SouthKorea) Wind tunnel experiments on Korean high speed trains using various ground simulation techniques. Journal of Wind Engineering and Industrial Aerodynamics 89 (2001) 1179-1195.

[4] E. Sabbioni, G. Tomasini (Department of Mechanical Engineering, Politecnico di Milano, Milano, Italy) Wind tunnel tests on heavy road vehicles: Cross wind induced loads. J. Wind Eng. Ind. Aerodyn. 99 (2011) 1011-1024.

[5] O.Meyer, W.Nitsche (Technical University of Berlin, Institute of Aero and Astronautics, Marchstr, Berlin, Germany) Update on progress in adaptive wind tunnel wall technology. Progress in Aerospace Sciences 40 (2004) 119-141.

[6] Giuseppe Pezzella, Edoardo Bucchignani (Centro Italiano Ricerche Aerospaziali, Via Maiorise, Capua CE, Italy) Numerical assessment of the flowfield features at the exit of Scirocco plasma wind tunnel

nozzle. Mathematics and Computers in Simulation 82 (2011) 118-131.

[7]  Yukio Tamura (Department of Architectural Engineering, Tokyo Polytechnic University, Atsugi, Kanagawa, Japan) Compensation of high frequency components of wind load by wind tunnel testing. J. Wind Eng. Ind. Aerodyne. 98 (2010) 929-935.

[8]  Venkat Lute , Akhil Upadhyay , K.K. Singh  (Civil Engineering Department, Indian Institute of Technology Roorkee, INDIA) Support vector machine based aerodynamic analysis of cable stayed bridges. Advances in Engineering Software 40 (2009) 830-835.

[9]  S. Kirschstein, W. Alles (Lehrstuhl für Flugdynamik, RWTH Aachen, Wüllnerstraße, Aachen, Germany) Identification of dynamic derivatives with a controlled wind tunnel model of the space plane configuration PHOENIX. Aerospace Science and Technology 8 (2004) 509-518.

[10]  Russell M. Cummings, Scott A. Morton, Stefan G. Siegel (Department of Aeronautics, United States Air Force Academy, USAF Academy, USA) Numerical prediction and wind tunnel experiment for a pitching unmanned combat air vehicle. Aerospace Science and Technology 12 (2008) 355-364

[11]  S. Rajakumar, Dr. D.Ravindran (Department of Mechanical Engineering, Anna University of Technology, Tirunelveli, Tamilnadu, India) Computational fluid dynamics of windturbine blade at various angles of attack and low reynolds number 2(11) (2010) 6474-6484

[12]  Kyoungwoo Park Juhee Lee (Department of Mechanical Engineering, Hoseo University, Chungnam, Republic of Korea) Optimal design of two dimensional wings in ground effect using multi objective genetic algorithm 37 (2010) 902-912

[13]  Karl Heinz Brakhage, Philipp Lamby (Institut für Geometrie und Praktische Mathematik, RWTH Aachen, Aachen, Germany) Application of B spline techniques to the modeling of airplane wings and numerical grid generation 25 (2008) 738-750

[14]  Jieun Song, Taehyoun Kim, Seung Jin Song (Department of Mechanical Aerospace Engineering, Seoul National University, Seoul, Republic of Korea) Experimental determination of unsteady aerodynamic coefficients and flutter behavior of a rigid wing  29 (2012) 50-61

[15]  Li Peifeng, Zhang Binqian, Chen Yingchun Yuan Changsheng (College of Aeronautics, Northwestern Polytechnical University, China) Aerodynamic Design Methodology for Blended Wing Body Transport. 25 (2012) 508-516

[16]  Dong Sun, Huaiyu Wu, Chi Ming Lam, Rong Zhu (Department of Manufacturing Engineering and Engineering Management, City University of Hong Kong, Kowloon, Hong Kong) Development of a small air vehicle based on aerodynamic model analysis in the tunnel tests  16 (2006) 41-49

[17]  A.R. Davari, M.R. Soltani (Department of Aerospace Engineering, Sharif University of Technology, Tehran, Iran) Effects of wing geometry on wing body tail interference in subsonic flow (2011) 18 (3) 407-415

[18]  J.J. del Coz Díaz, P.J. García Nieto (Department of Construction, University of Oviedo, Edificio Dep. de Viesques no 7, 33204, Spain) Numerical analysis of pressure field on curved self weighted metallic roofs due to the wind effect by the finite element method  192 (2006) 9, 40-50